CBN 99-32

Investigation of the feasibility of a free electron laser for the Cornell electron storage ring and linear accelerator

Marty Zwikel

Department of Physics, Grinnell College, Grinnell, IA, 50112

Abstract

Free electron lasers (FELs) constructed from storage rings and linear accelerators provide for strong, tunable sources of sub-visible wavelength coherent radiation. In this work we perform a one-dimensional simulation of a complete FEL oscillator for the 5 GeV Cornell electron storage ring (CESR) and the 350 MeV Cornell linear accelerator. We find viable storage ring FELs in the vicinity of 1.5 GeV beam energy and 50 nm output, and linac FELs around 320 MeV with 475 nm output. Both devices have a peak cavity power on the order of Watts.

Introduction

A free electron laser (FEL) essentially converts energy from a relativistic electron beam into coherent electromagnetic radiation [1]. By running an electron beam through a periodic undulator magnet, the electrons are accelerated in the transverse direction and will spontaneously radiate. A transverse energy modulation introduced by the undulator allows the radiation field to influence the beam, thereby extracting more energy from the electrons via stimulated emission. Given a long enough time scale, communication between the electrons will lead to an exponential growth in the radiation field.

The simulation code FELSim models the output radiation field and longitudinal electron trajectories of an arbitrary number of particles as they propagate through the system. We use actual beam parameters from CESR and the Cornell linac, as provided in the Appendix, to study the time evolution of the system. This simulation allows us to determine how variables such as beam emittance, energy spread, and sheer physical size constrain the complete parameter space of electron beam, undulator magnet, and output field in which a FEL might be constructed.

Theory of the Free Electron Laser Oscillator

The complete system we use in examining the FEL possibilities for the Cornell electron sources is shown in Fig. 1. Each device has key theoretical characteristics that must be elucidated in order to understand the simulation procedure. For a periodic planar undulator magnet of wavelength λ_u, magnetic field strength B, and an electron beam of relativistic gamma factor γ, the fundamental radiation wavelength at an angle of observation θ from the beam axis is given by:

$$\lambda_\gamma = \frac{\lambda_u}{2\gamma^2}(1 + \tfrac{1}{2}K^2 + \gamma^2\theta^2) \tag{1}$$

where K is the so-called undulator parameter, $K = 9.344\, B(\text{kG})\, \lambda_u(m)$. Calculations of the electron trajectories in the undulator reveal that a transverse velocity modulation occurs which allows for energy exchange with a co-propagating electric field [2]. To accurately model this system, we must apply a self-consistent approach of using the electron beam as a current source for the radiation

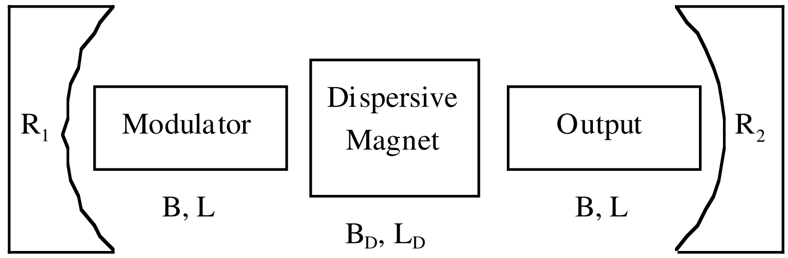

FIGURE 1. Schematic of a complete FEL oscillator. The electron beam enters at the modulator (undulator magnet) and exits after the output section.

field, and then letting this field act back on the electron beam. Murphy and Pellegrini derive the following set of equations to describe this process:

$$\dot{\psi}_j = \frac{1}{2\rho}\left(1 - \frac{1}{\rho^2 \Gamma_j^2}\right) \tag{2}$$

$$\dot{\Gamma}_j = \frac{-1}{\rho}\left[\frac{A}{\Gamma_j} e^{i\psi_j} + c.c.\right] \tag{3}$$

$$\dot{A} = \frac{1}{N_e} \sum_{j=1}^{N_e} \frac{e^{-i\psi_j}}{\rho \Gamma_j} \tag{4}$$

where *c.c.* indicates the complex conjugate, and N_e is the number of electrons. Differentiation in Eqs. 2-4 is with respect to the scaled time variable $\tau = (4\pi\rho c/\lambda_u)t$. Eqs. 2 and 3 are in fact $2N_e$ equations, a scaled phase and energy, respectively, for each electron. Eq. 4 describes the radiation field amplitude. Note that these equations have only one parameter, ρ, the so-called FEL parameter:

$$\rho = \left(\frac{K\lambda_u \Omega_p}{8\pi c\gamma}\right)^{2/3}, \text{where} \qquad \Omega_p = \left(\frac{2eI_{pk}}{m\gamma\sigma_r^2}\right)^{1/2} \tag{5}$$

is the electron beam relativistic plasma frequency, e and m are the electron charge and mass, c is the vacuum speed of light, I_{pk} is the peak current in amperes, and σ_r is the r.m.s. beam radius in meters. Table I provides a listing of the actual beam parameters used in simulation. The FEL parameter is a measure of the beam coupling to the radiation field, and goes inversely with γ, indicating lower coupling for high beam energies.

Table I. Storage ring and linac beam characteristics that contribute to the FEL parameter ρ. σ_s is the r.m.s. bunch length, I_b is the bunch current in the case of the storage ring, and the bunch intensity (in number of electrons) in the case of the linac, I_{pk} is the peak beam current, σ_r is the r.m.s. beam radius, and E is the beam energy. Ring values are produced for B = 4.0 kG, λ_u = 10 cm, and I_b = 20 mA. Linac values for 2.5 kG, 10 cm, and 2.5 x 10^{10} particles per bunch.

Parameter	Storage Ring		Linear Accelerator	
	Dependencies	Value at 1.4 GeV	Dependencies	Value at 0.3 GeV
σ_s	E	2 x 10^{-3} m	Constant	3 x 10^{-3} m
I_{pk}	σ_s^{-1}, I_b	3100 A	I_b	4400 A
σ_r	E	2.5 x 10^{-4} m	$E^{-1/2}$, I_b	1.1 x 10^{-3} m
ρ	See Page 2	1.2 x 10^{-3}	See Page 2	1.8 x 10^{-3}

As the system evolves, the electrons will begin to spread out in energy and bunch in phase with respect to the field. It is this bunching which allows for enhanced superposition of the emitted radiation, and a correspondingly high output power [1]. FELs may start up in one of two ways: a seed laser at the radiation wavelength can provide an initial field, or an initial bunching of the electron beam in the form of phase noise can be used. For sub-200 nm outputs, no seed lasers exist, and therefore startup from noise is the only option. The sheer physical size constraints of the magnets severely limits the optical gain of the undulator, so it is advantageous if some appreciable pre-bunching exists. An optical klystron (OK), a device composed of two undulators and a dispersive magnet (see Fig. 1) does just this. By converting the energy modulation introduced in the first undulator into a phase modulation on the optical wavelength, the beam is effectively pre-bunched and primed to radiate more strongly and quickly in the second undulator [3].

One final component of a FEL oscillator is the cavity end mirrors. For the electron beams in consideration, it became clear early on that a single pass system would not provide nearly enough output power, and thus a resonant cavity with round trip time equal to the electron pulse spacing is required. Materials with reflectances of 0.85 at wavelengths down to 10 nm have been manufactured, and could be used for the mirrors [4].

Simulation Input Parameters

The FELSim code is a simulation of the complete FEL oscillator described in the preceding section. An incoming electron bunch, or series of bunches, between 10^2 and 10^4 particles is inserted at the beginning of the modulation undulator and then run through the system over an arbitrary time interval. Each electron is assigned a phase and energy, so that the phase space is purely longitudinal. These two degrees of freedom do, however, allow for accurate simulation of beam energy spread and bunching. The electrons are initially distributed in pairs of the same energy, chosen at random from a Gaussian distribution, with phases given by:

$$\psi_{01} = 2\pi R \tag{6}$$

$$\psi_{02} = 2\pi R + \pi \tag{7}$$

where R is a random number between 0 and 1. This distribution technique cancels the shot noise which would occur in the small field regime due to inaccurate statistics, while still allowing the electrons to bunch and produce exponential field growth on longer time scales [5].

One two-dimensional effect, however, is particularly important to any FEL simulation – beam emittance. If the transverse beam size does not sufficiently overlap the optical mode, then there will be little energy exchange and optical gain. We can describe this problem onedimensionally as an effective energy spread that will reduce the gain for high emittances. Expanding Eq. 1 to lowest order in γ, K, and θ yields:

$$\frac{\Delta\lambda_\gamma}{\lambda_\gamma} \approx \frac{-2\Delta\gamma}{\gamma} + \frac{K\Delta K}{(1+\frac{1}{2}K^2)} + \frac{\gamma^2(\Delta\theta)^2}{(1+\frac{1}{2}K^2)} \tag{8}$$

If we define the beam emittance as $\varepsilon=\Delta\theta a$, where a is the maximum deflection amplitude along the undulator field axis, then the two rightmost terms become:

$$(\frac{\Delta\gamma}{\gamma})_{eff} = \frac{1}{(1+\frac{1}{2}K^2)}[\frac{K^2}{2}(\frac{2\pi}{\lambda_u})^2\frac{\lambda_\beta}{2\pi} + \frac{2\pi\gamma^2}{\lambda_\beta}]\varepsilon \tag{9}$$

where λ_β is the beta function of the undulator magnet. We take λ_β to be the "natural" beta function of the undulator, which is $\sqrt{2}\,\lambda_u\gamma/K$, so that:

$$(\frac{\Delta\gamma}{\gamma})_{eff} = \frac{\sqrt{8}\pi\gamma\varepsilon K}{\lambda_u(1+\frac{1}{2}K^2)} \tag{10}$$

We include this spread in our simulations, using the ring and linac emittances provided in Table II of the Appendix. Note that the linac emittance is rather poor, and yields an effective spread large compared to the coupling strength ρ. All linac simulations were conducted assuming an emittance 1/10 the current value, thereby avoiding this isolated problem [6].

Table II. Storage ring and linac beam energy spread and emittance effective energy spread contribution. ε is the beam emittance, and E is the beam energy. Emittance values are given in mrad mm.

Parameter	Storage Ring		Linear Accelerator	
	Dependencies	Value at 1.4 GeV	Dependencies	Value at 0.3 GeV
$(\Delta\gamma/\gamma)_{beam}$	E	1.7×10^{-4}	E^{-1}	2.2×10^{-3}
ε	E^2	3.2×10^{-9}	E^{-1}, I_b^2	8.1×10^{-8}
$(\Delta\gamma/\gamma)_{eff}$	ε, E	3.6×10^{-4}	ε, E	2.6×10^{-3}

An optical klystron is even more sensitive to energy spread, with an approximate acceptance given by the simple relation:

$$(G\frac{\Delta\gamma}{\gamma})_{OK} \approx (G\frac{\Delta\gamma}{\gamma})_{FEL} \tag{11}$$

It is inaccurate, however, to include the effective emittance spread in our klystron calculations, as the dispersive magnet performs an entirely different function than the undulator. In order to properly simulate a complete OK oscillator, one must use a three-dimensional simulation, which is beyond the scope of this work. We may still use an estimate of the ratio G_{OK}/G_{FEL} derived from low emittance simulations to obtain a rough prediction of the acceptance and gain for a given set of input parameters.

For a FEL/OK in a lossy resonant cavity, it is imperative that enough field remain in the cavity when the next electron bunch arrives. It has been determined via simulation that a gain per pass of unity is required early on to ensure an exponential buildup in the long run. As we increase the electron beam energy, eventually the gain per pass will reduce to unity. This energy defines the *critical gain* criteria of the system. Alternatively, when the energy spread effectively degrades the gain to unity, this energy defines the *critical spread* criteria of the system. For a given magnetic field, undulator wavelength, energy spread, beam intensity, and emittance, the *critical energy* is the lower of these two values, and defines the maximum beam operating energy for use in a FEL oscillator. The only difference between the storage ring and linac in this regard is that the linac can output 35 sequential bunches, while the storage ring can have 25 circulating bunches for the bunch intensities in consideration. After 35 passes of a linac oscillator, the field will simply decay to zero. Oscillations in the storage ring may continue indefinitely, although energy spread will accumulate within each bunch over time.

The parameters described above constitute the full input of the FELSim oscillator simulation. Fig. 2 shows the single pass evolution of the electron phase space and radiation field amplitude for a typical set of beam and magnet parameters. From $\tau = 0$ to $\tau = 1.22$ the beam is in the first undulator, which introduces an energy modulation. The dispersive magnet slews the phase space in a relatively short amount of time, which then allows for exponential buildup in the output undulator. In considering the entire parameter space of which a FEL can be chosen, however, we cannot simulate every possible system due to computation time constraints. Instead we employ the small signal gain result of Murphy and Pellegrini to determine the gain per pass of an undulator starting from some small initial field [7]. This approximation may then be used with the gain and spread criteria described earlier to determine a given system's critical energy. The full set of critical energies and input parameters constitutes the complete parameter space of viable FELs. A detailed simulation of an attractive system is then performed to accurately determine the output field behavior and peak cavity power.

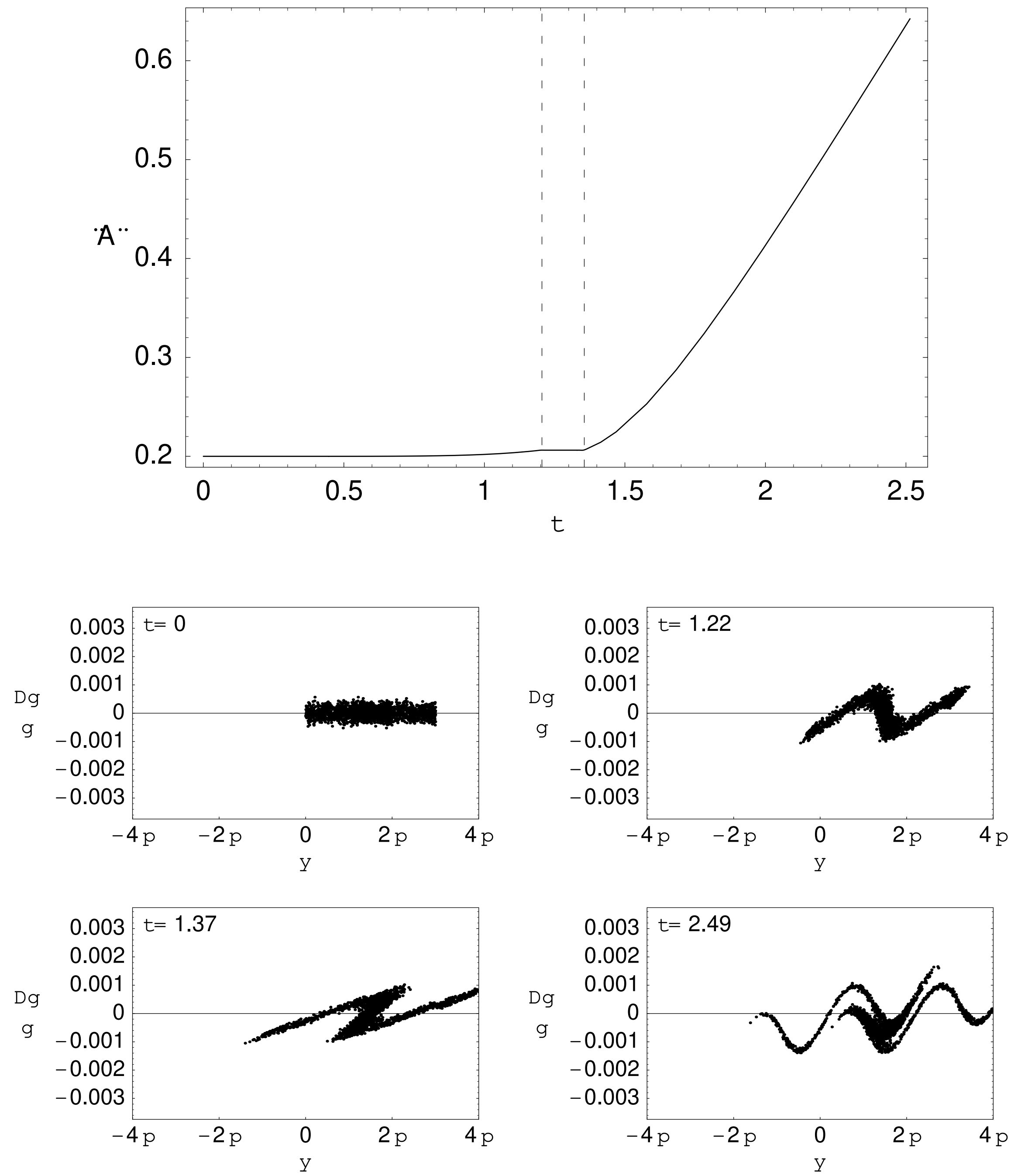

FIGURE 2. Typical FEL oscillator single-pass simulation conducted with 2,000 electrons. The radiation field amplitude |A| is given a large initial value of 0.2, as might be the case after field buildup over a number of passes, to demonstrate the effect of the dispersive magnet more clearly. The dashed lines on the field plot indicate the start and end of the dispersive magnet. The lower figures illustrate the evolution of the electron longitudinal phase space.

Results

Figs. 3 and 4 illustrate the parameter space from which a storage ring or linac FEL can be constructed. The upper plots in each figure fix the bunch current or intensity, and undulator parameters, to show where the gain and spread criteria limit the choice in beam energy. The lower of these values is the critical energy for a given parameter set, and this quantity is plotted for a number of magnetic field contours in the lower plots. One may then simply pick a point on any contour for simulation, as this represents a viable FEL oscillator.

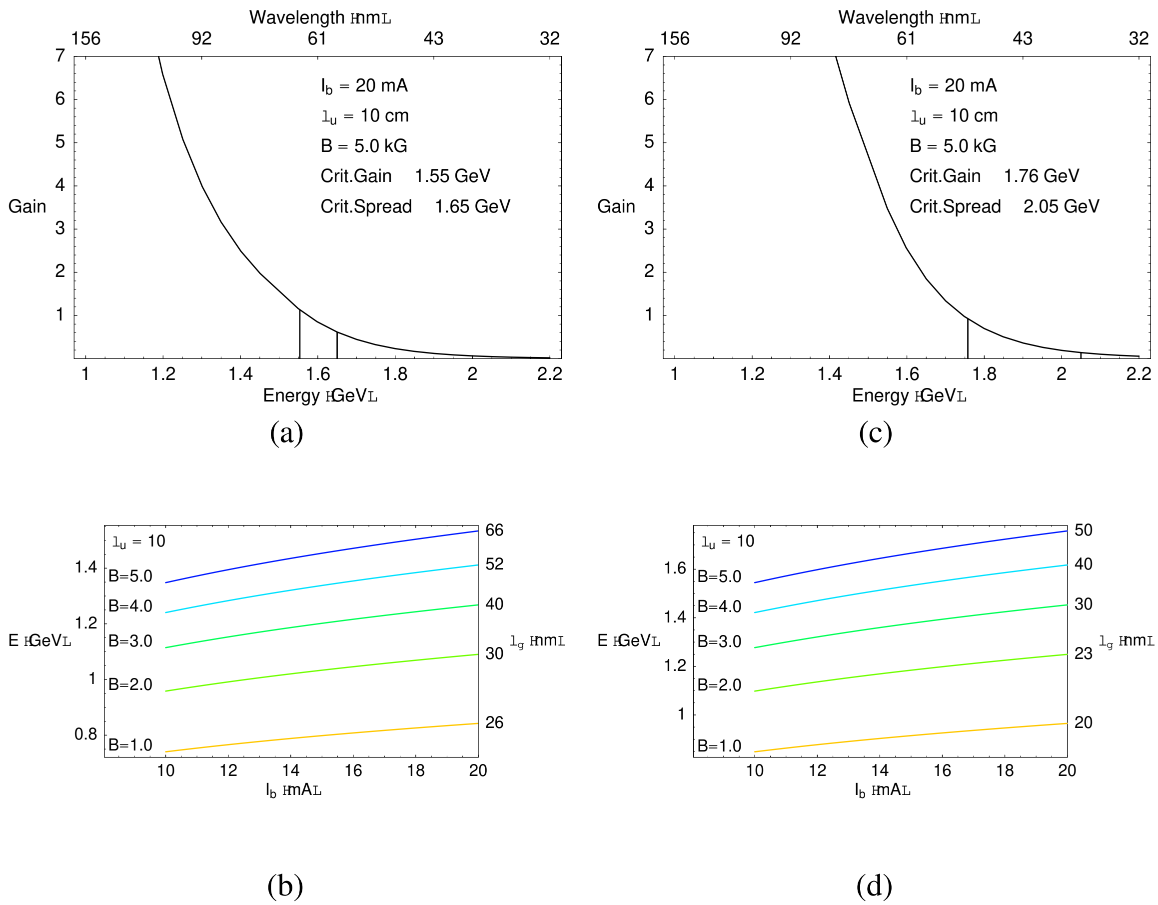

FIGURE 3. Parameter space for storage ring FEL oscillators. Figs. 3a & 3b show the parameter space for a single 15m undulator, while Figs. 3c & 3d describe an OK with a pair of 7.5m undulators and a 1m dispersive magnet. The upper plots illustrate the critical gain and spread criteria for a particular system, and the lower plots show various critical energy contours for different undulator magnetic field settings. λ_u is presented in cm, and B in kG.

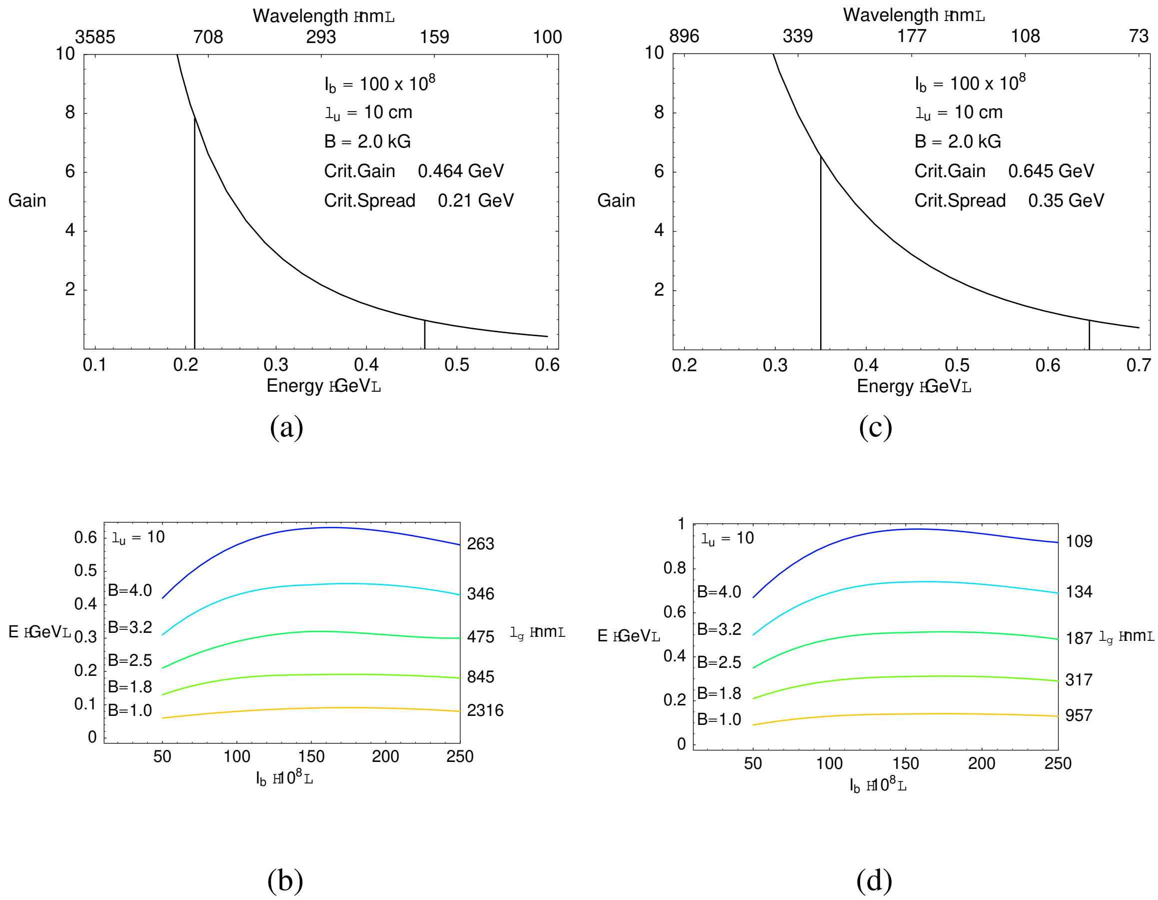

FIGURE 4. Parameter space for linac FEL oscillators. Figs. 4a & 4b show the parameter space for a single 15m undulator, while Figs. 4c & 4d describe an OK with a pair of 7.5m undulators and a 1m dispersive magnet. The upper plots illustrate the critical gain and spread criteria for a particular system, and the lower plots show various critical energy contours for different undulator magnetic field settings. λ_u is presented in cm, and B in kG.

Note that in both the storage ring and linac cases, the optical klystron system allows for use of beam energies roughly 200 MeV greater than would be possible with a single undulator of the same length. This in turn lowers the output radiation wavelength as well as the magnetic field required to obtain such an output.

The contour plots for each electron source have qualifications that must be noted here. In the case of the storage ring, the beam must be operated at an energy greater than 1 GeV, and possibly even greater than 1.5 GeV, to avoid beam decay via the Touschek effect [8]. Conversely, the linac cannot be operated at an energy much greater than 350 MeV. To reach higher energies, the beam could be accelerated somewhat in the Cornell synchroton. This, however, will increase the beam emittance and reduce gain at some point as well. Thus it is suggested that 400 MeV is the maximum linac FEL energy.

We now choose particular storage ring and linac systems from these contours and perform a high quality simulation of 2,000 electrons. The radiation field amplitudes presented in Figs. 5 & 6 reach maximum values near unity, a result that is found to be independent of undulator or beam parameters. The cavity power at this saturation value then depends only on the undulator parameter K and the FEL parameter ρ. For both simulations conducted we find a peak of approximately 6

Watts, an impressive amount of power in the tens of nm regime of our storage ring FEL, and still a significant value for the visible linac FEL. Examination of the OK contours for each electron source reveals that even lower wavelengths can be obtained, and from a theoretical standpoint these systems should achieve the same cavity power at their critical energies. We cannot, however, simulate the complete OK oscillator using the one-dimensional FELSim code, but the results indicate that wavelengths in the ultraviolet are within the reach of a Cornell linac FEL.

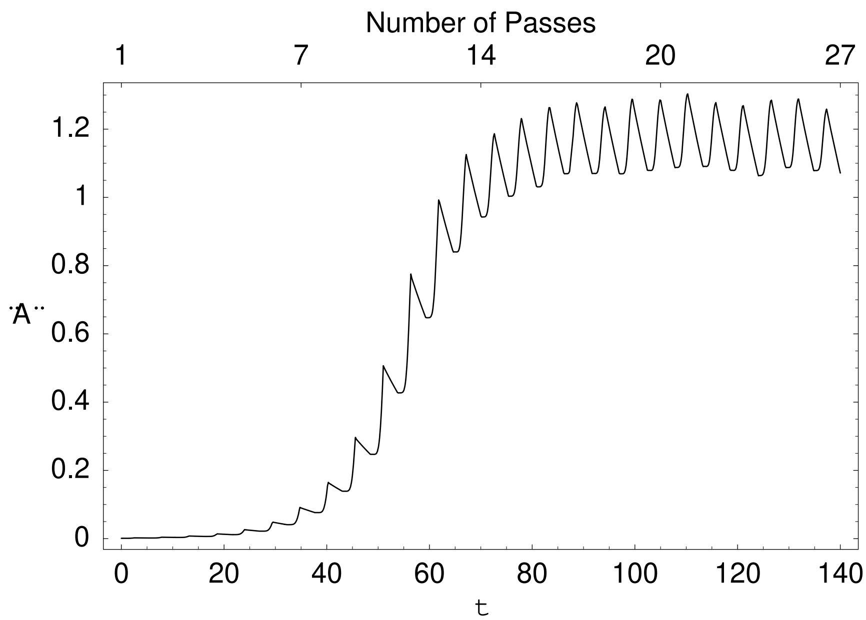

FIGURE 5. Radiation field amplitude for a 15m FEL in a 17m cavity. Mirror reflectances are R_1=R_2=0.85. Simulation was conducted with: E = 1.4 GeV, λ_u = 10 cm, B = 4.0 kG, I_b = 20 mA. Radiation wavelength is 52 nm.

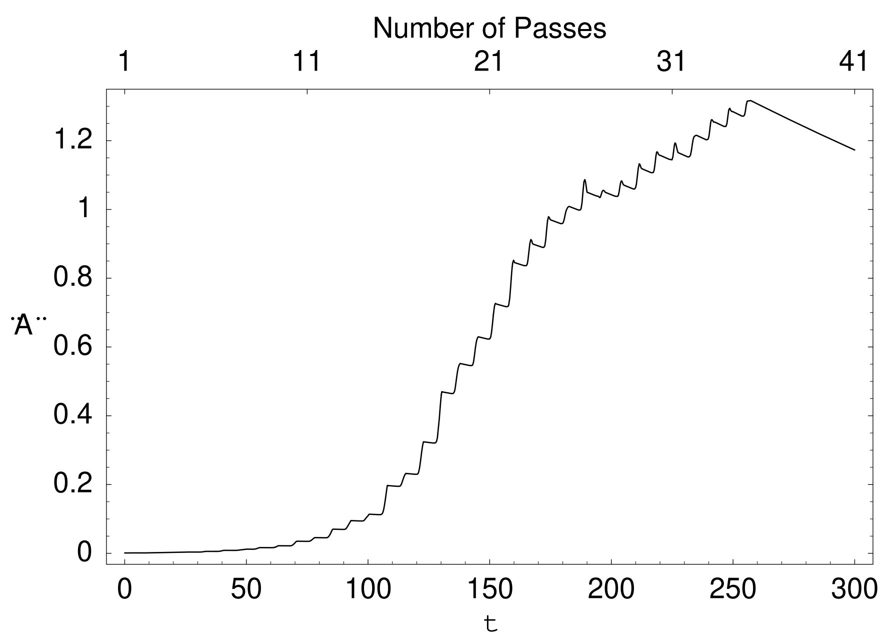

FIGURE 6. Radiation field amplitude for a 15m FEL in a 17m cavity. Mirror reflectances are R_1=0.98, R_2=1.0. Simulation was conducted with: E = 320 MeV, λ_u = 10 cm, B = 2.5 kG, I_b = 2.5 x 10^{10} electrons. Radiation wavelength is 475 nm.

Conclusions

Both the Cornell electron storage ring (operating at 1.4 – 1.8 GeV) and linear accelerator (with an improved electron injector) make quite feasible electron sources for powerful sub-visible wavelength FELs. Using the FELSim simulation code, we have identified regions of the complete parameter space of the beam-oscillator system in which a FEL oscillator could be constructed, and have simulated attractive systems for both electron sources. We find a storage ring FEL in the vicinity of 50 nm and a linac FEL in the visible or SUV regime, with peak cavity powers of approximately 6 Watts. Use of an optical klystron is shown to allow for even lower wavelength operation at a similar power output.

Acknowledgments

The author would like to thank Professor Gerry Dugan of Cornell University, who proposed this Research Experience for Undergraduates project, for his help in understanding the free electron laser and for his guidance in the simulation coding and analysis.

This work was supported by the National Science Foundation REU grant PHY-9731882 and research grant PHY-9809799.

Footnotes and References

1. J.B. Murphy and C. Pellegrini, "Introduction to the Physics of the Free Electron Laser," in Lecture Notes in Physics 296, M. Month and S. Turner, eds., p. 163.
2. H. Wiedemann, Particle Accelerator Physics II, (Springer, Berlin, 1995), p. 400.
3. R.H. Pantell, "Free Electron Lasers," in AIP Conference Proceedings 184, M. Month and M. Dienes, eds., p. 1718.
4. R.L. Johnson, "Grating Monochromators and Optics for the VUV and Soft X-Ray Region," in Handbook on Synchrotron Radiation, Volume 1A, E. Koch, ed., p. 177.
5. C. Brau, "Free Electron Lasers," in AIP Conference Proceedings 184, M. Month and M. Dienes, eds., p. 1689.
6. Implementation of a more modern electron gun should decrease the linac beam emittance by the required order of magnitude.
7. While we are interested in startup from noise, this is difficult to simulate due to the relatively small number of particles in consideration. We thus assume a very small initial field, one that would certainly develop from noise after the first pass in an oscillator.
8. Aipiwinski, "Touschek Effect and Interbeam Scattering," in Handbook of Accelerator Physics and Engineering, Tigner and Chao, eds., p.125.